

Received 27 April 2023, accepted 18 May 2023, date of publication 24 May 2023, date of current version 5 June 2023.

Digital Object Identifier 10.1109/ACCESS.2023.3279721

## RESEARCH ARTICLE

# Wideband Bandpass TM Cavity Filters With Wide Spurious Free Band

ABDUL REHMAN<sup>1</sup> AND CRISTIANO TOMASSONI<sup>1,2</sup>, (Senior Member, IEEE)

<sup>1</sup>Electronic and Information Engineering Department, University of Perugia, 06125 Perugia, Italy

<sup>2</sup>Consorzio Nazionale Interuniversitario per le Telecomunicazioni (CNIT), 43124 Parma, Italy

Corresponding author: Abdul Rehman (abdul.rehman@unipg.it)

This work was supported by the European Union's Horizon 2020 Research and Innovation Program funded by the Marie Skłodowska-Curi under Grant 811232-H2020-MSCA-ITN-2018.

**ABSTRACT** Recently, the spurious self-suppression method has been introduced and applied to the bandpass TM cavity filters to improve their stopband performance. However, this method has the limitation of being applicable only to TM narrow-band filters. This paper shows how to overcome this limitation. In particular, it shows how to increase the bandwidth and improve the stopband performance by removing the spurious resonance of the coupling irises due to  $TE_{10}$  mode. The conventional rectangular iris is replaced by a new bent c-shaped iris. In this way, the resonance of the iris  $TE_{10}$  mode can be shifted to lower frequencies (below the cut-off), improving the stopband performance of the filter. Moreover, this new iris shape provides large couplings that allow wide passbands, and strong excitation of the spurious resonant modes that allows for an efficient implementation of the spurious self-suppression method. Furthermore, double slot iris has been used to connect the two central cavities to increase the central coupling of the filter. Design examples of 4<sup>th</sup> order and 6<sup>th</sup> order TM cavity filters with wide spurious free range up to 18 GHz having fractional bandwidth (FBW) of 5% and 4%, respectively, are presented. Finally, the 6<sup>th</sup> order TM cavity filter has been manufactured and measured. Good agreement has been achieved between simulated and measured frequency responses.

**INDEX TERMS** Bandpass filters, bent c-shaped iris, coupling irises, higher order modes, out-of-band, spurious self-suppression, transverse magnetic (TM) cavity.

## I. INTRODUCTION

The rapid technological advancement demands for microwave/millimeter wave components with stringent requirements as for example compact size, and wide out-of-band rejection performance. Microwave filters is one of the key components in communication systems and must meet such stringent requirements [1], [2]. Waveguide filters have been extensively used in communication system, especially in satellite applications, thanks to their low loss characteristics and high-power handling capabilities [3], [4]. An important parameter to be considered in the design of bandpass filters is their out-of-band rejection response. Bandpass filters in rectangular waveguide technology often suffer from spurious

resonances that limit the wideness of their stopbands. In particular, higher order modes in a resonator create spurious resonances and limit the stopband performance of the rectangular waveguide filters. The improvement in the stopband performance has been traditionally obtained by cascading a lowpass filter to a bandpass filter [5]. However, it increases design complexity and overall size of the whole structure. Another intuitive approach recently proposed in [6], uses a rearranged position of filter cavities. The proposed arrangement allows minimizing coupling values to spurious modes. However, in some cases, coupling values can be minimized but cannot be avoided due to manufacturing tolerances and this results in the appearance of very narrow-band spurious resonances degrading the out-of-band frequency response of the filter. Other solutions, exploiting stepped-impedance resonators (SIRs) and resonators with

The associate editor coordinating the review of this manuscript and approving it for publication was Muhammad Usman Afzal<sup>1</sup>.

different widths to improve out-of-band performance in rectangular waveguide bandpass filters, have been reported in [7] and [8]. Despite achieving better stopband performance, this results in increased manufacturing cost and design complexity. Recently, out-of-band performance of SIR based filters has been improved by providing a hybrid solution using capacitive and inductive irises [9], [10]. The study has been extended in [11], where a staircase solution has been proposed. In this case, wideband filters with wide out-of-band regions have been obtained at the expense of complex design and manufacturing process.

The use of transmission zeros (TZs) is another technique to improve filter selectivity and its out-of-band frequency response. Multiple coupling path solution which makes the use of cross-couplings between non-adjacent resonators has been used in [12] to generate TZs. In [13], out-of-band performance has been improved by using higher order modes to generate TZs. In [14] and [15], TZs has been introduced and placed far away from the filter passband with the use of cross-couplings between non-adjacent resonators which results in a folded configuration. However, these approaches do not consider suppression of higher order modes spurious frequencies.

The use of transverse magnetic (TM) mode combined with the use of non-resonating modes, allows for filter miniaturization and for filter selectivity improvement, thanks to the introduction of TZs [16], [17]. Different TM cavity filter configurations, including dual mode configurations, have been used in [18] and [19]. In [20], a compact waveguide bandpass filter using TM dual mode cavities achieving fractional bandwidth (FBW) of 3.5% has been designed, measured, and tested. Despite achieving excellent performance in terms of selectivity, TM filters often suffer from poor out-of-band rejection performance. In the context of TM mode cavities, two types of spurious resonances have been identified: higher order cavity mode resonances and coupling iris resonances. Such additional spurious resonances create parasitic bands that can degrade the stopband performance of the TM mode filters. In [21], out-of-band behavior in TM dual mode cavities is improved by using multiple irises and modifying the shape of cavities.

Recently, a new method called spurious self-suppression has been proposed in [22] and [23]. In [24], it has been applied to substrate-integrated waveguide (SIW) filters. This method is different from the classical one [6], which consists in the minimization of all possible couplings to spurious resonances, with the aim of avoiding (or better saying limiting) the excitation of spurious modes. The limitations of [6] were also addressed in [23], by providing example of TM mode filters. Another possible limitation of TM mode filters could be their limited bandwidths, especially when wide stopbands are required and the spurious self-suppression method is applied, as can be seen in the examples provided in [23]. Although recent studies [25] and [26] show, it is possible to achieve wide passbands up to 9.33% in TM cavity filters, using resonant irises and direct coupled TE-TM waveguide

cavities. However, both these studies do not consider the wide out-of-band frequency response of the filter. In addition, the use of resonant irises results in compromising the Q factor of the overall structure [25].

Keeping in mind the limitations of the different filter technologies discussed above, this paper extends the previous contribution presented in [23] about TM mode filters designed by exploiting the spurious self-suppression method. In particular, in this paper the limited capability in terms of the bandwidth related to the structures presented in [23] has been addressed by introducing new iris geometries that allow filters with wider passbands. The bandwidth increasing in TM filters related to the structures presented in [23], creates spurious frequencies due to the iris resonances close to the filter passband. The two major contributions here in this paper introduced, consist in:

- 1) Removing spurious frequencies, due to the resonance of the TE<sub>10</sub> mode of coupling irises, by replacing the conventional rectangular iris with a new bent c-shaped iris. This results in improving the stopband performance of the filter.

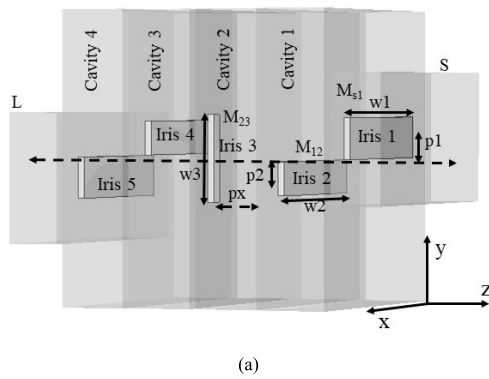
- 2) Increasing the bandwidth in wide spurious free TM cavity filters. With the presented structures, bandwidths of up to 5% are obtainable while in [23], the limit was about 1.5%.

This paper is organized as follows. In Section II, the problem in increasing the bandwidth using the spurious self-suppression method in TM cavity filters has been addressed. In Section III, detailed analysis on how to increase the bandwidth and enhance the stopband frequency response in TM cavity filters is presented. Examples of 4<sup>th</sup> order and 6<sup>th</sup> order TM cavity filters have been presented in this section. Section IV shows the measured results of the 6<sup>th</sup> order TM cavity filter. Measurement of the 6<sup>th</sup> order TM cavity filter confirms the feasibility of the proposed approach. Finally, the conclusion is presented in Section V.

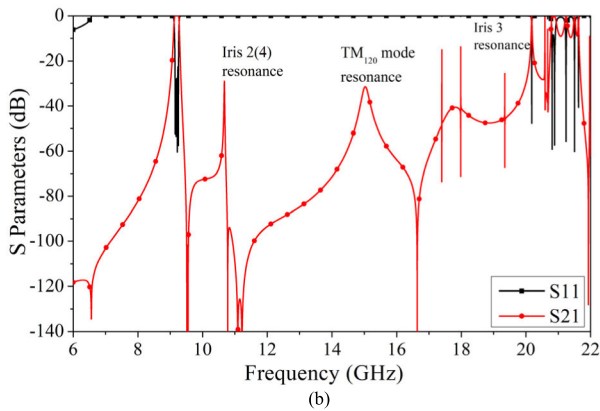
## II. STUDY OF THE BANDWIDTH ENHANCEMENT IN WIDE SPURIOUS FREE BAND TM CAVITY FILTERS

The idea of controlling spurious resonances through their coupling values (with the spurious self-suppression method) has been presented in [22] and [23]. For the sake of simplicity, results of the 4 pole TM cavity filter have been here recalled. Fig. 1(a) shows the configuration of the 4<sup>th</sup> order TM cavity filter, and its wide spurious free band frequency response is shown in Fig. 1(b) [23]. The filter has a FBW of 1.3% and the first spurious resonance appears at around 20.2 GHz (iris 3 resonance), achieving stopband up to 2.2 times the filter center frequency of 9.2 GHz. Iris 2 (4) resonances appears instead at 10.65 GHz but with an insertion loss of 30 dB. The filter is fed through standard *wr-90* waveguides with a cut-off frequency of 6.557 GHz. Note that, the range of the graph also includes frequencies below the cut-off frequency.

The classical approach for increasing the bandwidth in single mode TM filters, consists in increasing iris sizes or increasing the distance between irises and the cavity center in order to increase the coupling values [17], [18], [19]. However, in both cases, stopband performance is degraded.



(a)



(b)

FIGURE 1. Four pole TM cavity filter. (a) Filter configuration. (b) S-parameter response reported in [23].

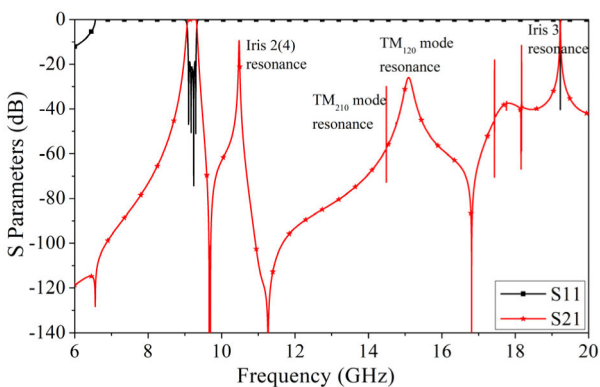


FIGURE 2. S-parameter response of increasing bandwidth (2.2%) by increasing iris sizes  $w_1$ ,  $w_2$ ,  $w_3$  and iris distances  $p_1$ ,  $p_2$ ,  $p_x$  from the cavity center.

Fig. 2 shows the frequency response when bandwidth is increased up to 2.2% by increasing iris sizes ( $w_1$ ,  $w_2$ ,  $w_3$ ) and iris distances ( $p_1$ ,  $p_2$ ,  $p_x$ ) from the cavity center. Stopband performance degradation is clearly visible. In particular, the insertion loss of the resonance of the iris 2 (4) decreases to 10 dB (in Fig. 1(b), it was instead 30 dB). In addition, this resonance become close to the filter passband at around 10.48 GHz (in Fig. 1(b) it was instead at 10.65 GHz). Both these stopband performance degradation effects are due to the increase in iris size  $w_2$ . Increasing  $w_3$  also contributes to

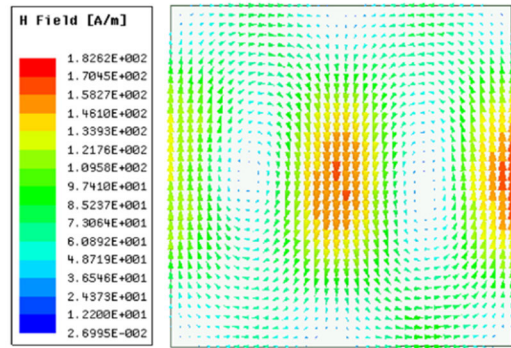


FIGURE 3. The magnetic field of the  $TM_{210}$  mode calculated at 14.48 GHz.

increasing iris 2 (4) spurious level. Note that, according to the spurious self-suppression method, higher attenuation can be obtained for iris resonances when the central iris (iris 3) resonates far away from the iris parasitic band [23].

Similarly, increasing  $w_3$  results in increasing higher order mode  $TM_{120}$  spurious band level and its insertion loss reaches 25 dB. Additionally, as a result of increasing  $w_3$ , the  $TM_{210}$  cavity mode also produces resonance at 14.48 GHz reaching the level of 30 dB. Fig. 3 shows the magnetic field calculated at 14.48 GHz. This corresponds to the field of the  $TM_{210}$  mode, thus demonstrating that the spurious resonance at 14.48 GHz is due to that mode. Central iris 3 resonance is now present at 19 GHz. Obviously, further bandwidth increasing using this approach (increasing  $w_2$  and  $w_3$ ) will result in a further degradation of the stopband filter frequency response.

### III. FILTER DESIGNS WITH WIDE BANDWIDTH AND IMPROVED STOPBAND FREQUENCY RESPONSES

In order to increase the filter bandwidth avoiding stop-band performance degradation, a new approach is proposed in this paper. This new approach consists in two steps: 1) Increasing the electrical length of the iris 2 (4) (modifying width  $w_2$  of the straight iris) to lower the resonance frequency of the  $TE_{10}$  mode iris resonance. 2) Using the double slot iris in the two central cavities with the two slots symmetrically placed with respect to the cavity center. In the following, we will study the effect of this new approach to the frequency response of 4<sup>th</sup> order and 6<sup>th</sup> order TM cavity filters.

#### A. 4<sup>th</sup> ORDER FILTER DESIGN

The design of this filter is shown in two steps:

- 1) INCREASING THE ELECTRICAL LENGTH OF THE IRIS 2 (4) (MODIFYING WIDTH  $w_2$  OF THE STRAIGHT IRIS) TO LOWER THE RESONANCE FREQUENCY OF THE  $TE_{10}$  MODE IRIS RESONANCE

In the first step, conventional rectangular iris is replaced by an iris with an increased electrical length leading to the new bent c-shaped iris of Fig. 4. This results in shifting iris resonance to lower frequencies (below the cut-off of the feeding

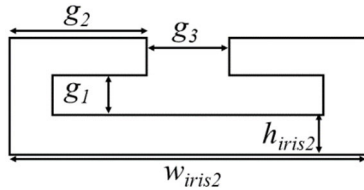


FIGURE 4. New bent c-shaped iris to control  $TE_{10}$  mode resonance.

waveguides, 6.557 GHz), thus improving the stopband performance of the filter. The schematic modal field distribution of the E-field for the  $TE_{10}$  and  $TE_{30}$  iris modes are shown in Fig. 5(a) and Fig. 5(b), respectively. The reason why the iris is bent is because this allows a better control of the coupling. Indeed, it is also possible to increase the iris size ( $w_2$ ) of a straight iris for obtaining iris resonance frequencies below the cut-off of the feeding waveguides. However, in this case the coupling level obtained by such irises is too high. In order to lower it at the needed levels, it is necessary to decrease very much the iris height  $h_{iris}$ , this will result in the impossibility of manufacturing it. Another way to lower the coupling value is instead to bend the iris, and this is the approach we followed.

In conclusion, with the proposed iris, we obtain two results: iris resonance frequency below the cut-off of the feeding waveguides and an increased coupling value to obtain wider bandwidth. However, the coupling cannot be too high, and its level is controlled by bending the iris. Indeed, according to Fig. 5(a), in the bent part of the iris the electric field has an opposite direction with respect to the field in the central part of the iris, and it contribute to decrease the coupling. This iris also allows a large coupling to higher order modes ( $TM_{120}$ ). This allows us to use the spurious self-suppression method [22], [23]. As according to this method, all couplings to the spurious modes need to be maximized except the central one.

Fig. 6 shows how to remove the spurious resonance of iris 2 (4) at 10.48 GHz, by increasing the electrical length of the iris and by bending it. Step #1 (black curve) is that of Fig. 2 referred to the structure of Fig. 1(a) with straight iris. In this case, iris 2 (4) resonates above the passband at 10.48 GHz. Step #2 and step #3 instead show the  $S_{21}$  responses with the new bent c-shaped iris of Fig.4, where iris resonates below the passband, thanks to the increased iris electrical length. In particular, step #2 (red curve) shows the iris resonance just above the cut-off frequency (6.557 GHz). Step #3 (blue curve) instead has been obtained further increasing the iris electrical length and it shows the  $S_{21}$  response when iris resonance is below the cut-off and the resonance disappears. Step #2 and step #3 are achieved by using the parameter ( $g_3$ ) to control the coupling and the parameter  $w_{iris2}$  to readjust the iris resonance. Fig. 7 shows the frequency response obtained after step #3 with the new bent c-shaped iris, where the filter achieved FBW of 2.2%. Based on the modal field distribution of the  $TE_{10}$  mode (Fig. 5(a)), this new iris shape provides large  $M_{12}$  coupling. Much larger than that obtained with the conventional rectangular iris of Fig. 1(a). To decrease its

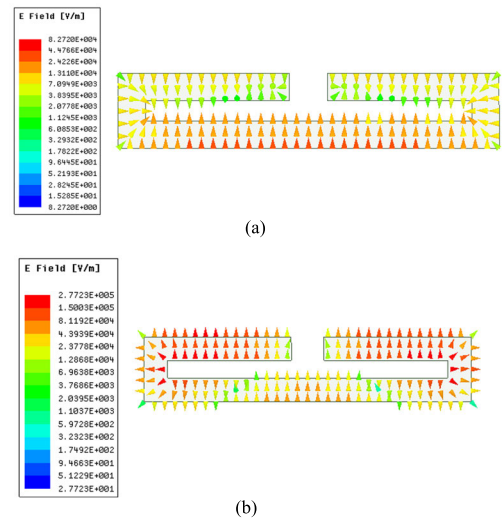


FIGURE 5. Field distribution in the bent c-shaped iris. a) E-field of the  $TE_{10}$  mode. b) E-field of the  $TE_{30}$  mode.

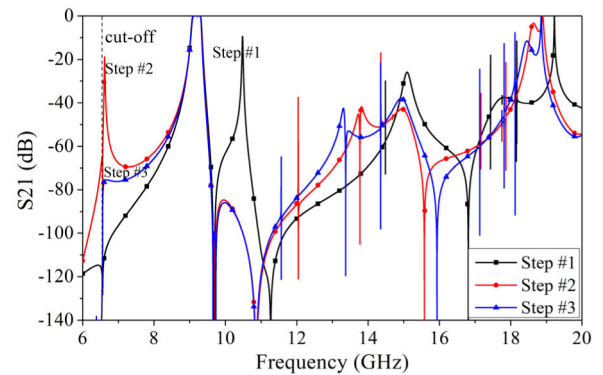


FIGURE 6. Removing  $TE_{10}$  mode iris resonance by increasing the iris electrical length. Step #1 (straight iris),  $w_{iris2} = 14.48$  mm,  $h_{iris2} = 2.6$  mm; Step #2,  $w_{iris2} = 13.95$  mm,  $h_{iris2} = 1$  mm,  $g_1 = 0.75$  mm,  $g_2 = 5.775$  mm,  $g_3 = 2.4$  mm; Step #3,  $w_{iris2} = 13.95$  mm,  $h_{iris2} = 1$  mm,  $g_1 = 0.75$  mm,  $g_2 = 6.275$  mm,  $g_3 = 1.4$  mm.

value and to recover the desired  $M_{12}$ , the new bent c-shaped iris is placed close to the cavity center ( $p_2 = -0.2$  mm). Indeed, the closer the iris to the cavity center, the lower the coupling  $M_{12}$ . On the other hand, the closer the iris to the cavity center, the higher the coupling to the higher order modes [23].

This mechanism allows independent control of both the couplings,  $M_{12}$  and coupling to higher order modes  $TM_{120}$ . Indeed, in order to increase the coupling to higher order modes while maintaining the same value of  $M_{12}$ , it is possible to proceed with the following two steps: a) Increase the iris electrical length in order to increase the value of both couplings, b) Decrease the distance of the iris from the cavity center in order to decrease the coupling value  $M_{12}$  until the original value is restored. This results in an increased coupling to higher order modes, as required by the spurious self-suppression method, where all couplings must be maximized except the central one [22], [23]. The parasitic band related to the  $TM_{120}$  modes is now more attenuated, reaching the level

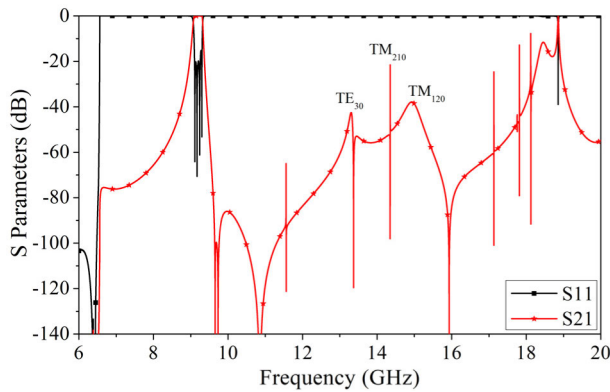


FIGURE 7. Filter S-parameters response with the new bent c-shaped iris.

of 40 dB. Note that this new iris also produces resonance due to TE<sub>30</sub> mode (Fig. 5 (b)). However, this resonance is far from the filter passband. It is positioned around 13.3 GHz with an insertion loss of below 40 dB as shown in Fig. 7. The spike appearing at 14.3 GHz reaches the level of 20 dB is due to the TM<sub>210</sub> mode present in the cavity. Other higher order mode (TM<sub>220</sub>) resonances in the cavity are present around 17/18GHz. However, as shown later on, these resonances can be removed by using the double slot iris in the central cavities.

2) DOUBLE SLOT IRIS IN THE CENTRAL CAVITIES

Fig. 8(a) shows the front view of the central iris with two symmetrical slots. The two slots are identical and symmetrically placed with respect to the cavity center. Doubling the slots results in two advantages. a) Increases the coupling  $M_{23}$  while maintaining the same frequency of the spurious related to the slot resonances. b) Avoids the excitation of the TM<sub>210</sub> higher order mode of the cavity, thanks to the symmetrical excitation of the fields made by the double slots.

Fig. 8(b) shows the frequency response of the filter obtained after using the double slot iris. The filter in-band frequency response remains the same as of that in Fig. 7, but the central iris resonance is now pushed at the higher frequencies (20.3 GHz). This is because the coupling obtained with a single slot iris can be obtained with smaller slot width ( $w_{iris3}$ ) in a double slot iris. Furthermore, thanks to the symmetric excitation of the double slot iris, the spurious related to the TM<sub>210</sub> mode is disappeared.

By applying the method illustrated above, it is possible to design wide band TM filters. Fig. 9(a) shows the structure of a 4<sup>th</sup> order TM cavity filter with FBW of 5%. Its frequency response is shown in Fig. 9(b). The desired coupling between source and cavity 1 ( $M_{s1}$ ) is obtained by properly selecting the parameters of iris 1 (increasing  $p_1$ ,  $w_{iris1}$ ).  $M_{12}$  can be obtained by increasing the distance  $p_2$  of the bent c-shaped iris (iris 2) from the cavity center and properly selecting the iris parameters defining its electrical length ( $g_1$ ,  $g_2$ ,  $g_3$ ,  $w_{iris2}$ ), and  $h_{iris2}$ .  $M_{23}$  can be obtained by increasing the distance  $p_x$  from the cavity center and the size  $w_{iris3}$  of the two central irises. The TE<sub>30</sub> mode iris resonance is present at

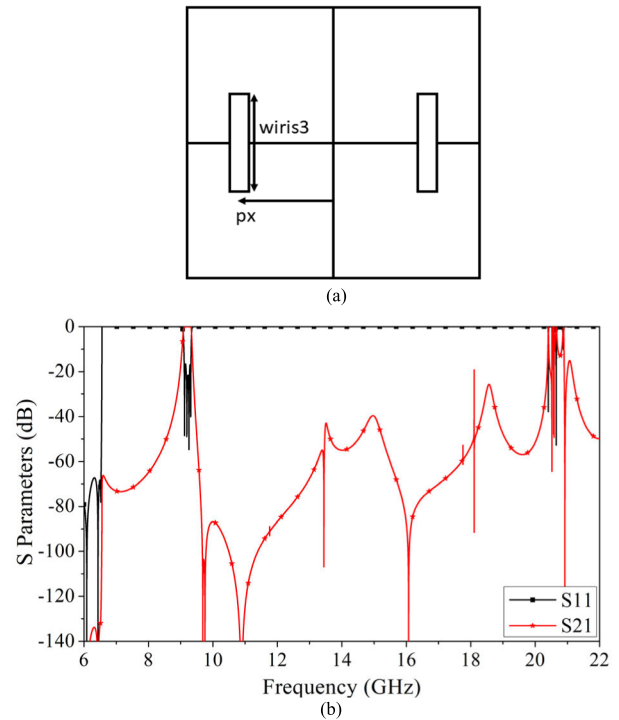


FIGURE 8. Filter with double slot iris. (a) Front view of the double slot iris. (b) Frequency response of the filter with double slot iris.

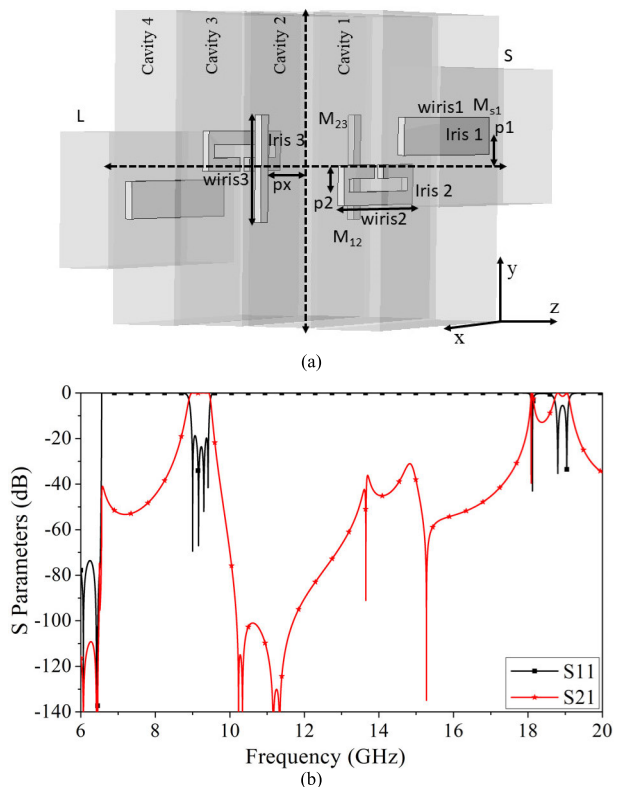


FIGURE 9. Four pole TM cavity filter. (a) Final configuration. (b) S-parameter response with wide FBW of 5%.

around 14 GHz with an insertion loss of 35 dB. The higher order TM<sub>120</sub> mode spurious level is 32 dB and is present

at around 15 GHz. Note that, the double slot iris increases the  $TM_{120}$  mode parasitic band level. However, thanks to the large coupling of bent c-shaped iris to the  $TM_{120}$  spurious mode, it is well suppressed up to 32 dB. The central iris resonance is at 18 GHz. The filter bandwidth obtained with the proposed method (5%) is much higher than that obtained (1.3%) by using the method illustrated in [23].

**B. 6<sup>th</sup> ORDER FILTER DESIGN**

In order to show the effectiveness of the proposed method to higher order filters, a 6<sup>th</sup> order TM cavity filter has been designed. Similar steps reported above for the 4<sup>th</sup> order filter have been followed and applied to the design of the 6<sup>th</sup> order filter to remove coupling iris resonances due to  $TE_{10}$  mode and increasing the bandwidth.

The configuration of the final 6<sup>th</sup> order TM cavity filter with the new bent c-shaped irises is shown in Fig. 10 (a). The filter is fed through standard  $wr-90$  waveguides. As reported in [23], to control the positioning of TZs below and above the passband, structure with antisymmetric positioning of irises is selected. In this case, irises 1 and 2 are placed both above the cavity center, whereas irises 6 and 7 are placed both below the cavity center. Similarly, irises 3 and 5 are placed one below and the other above the cavity center. Cavities 1 and 6 produces a double TZ at the lower stopband whereas cavities 2 and 5 produces two closely placed TZs at the upper stopband. The two zeros in the upper stopband are clearly visible. The corresponding S parameters response is shown in Fig. 10(b). Spurious resonances related to the  $TE_{10}$  mode of the irises 2, 3 (5 & 6) have been removed by increasing the irises electrical lengths and by using the bent c-shaped irises, according to the procedure illustrated for the design of the 4<sup>th</sup> order filter. They are all below the cut-off frequency (6.557 GHz) of the  $wr-90$  feeding waveguides. Resonance due to the central double slot iris (iris 4) resonates at higher frequencies along with other spurious resonances. The FBW of the filter is 4%. The FBW of the filter can be improved up to 5%, but at the expense of a small degradation of the stopband. Indeed, according to the authors experience, further increase in the FBW will result in the stopband performance degradation as increasing of the central coupling value requires increasing the size of double slot iris (iris 4 in this case). This will result in decreasing its resonance frequency thus reducing the band of stopband region.

The  $TE_{30}$  mode of the irises resonates at 12.8 GHz and 13.5 GHz and their insertion loss is 12 dB and 30 dB, respectively. However, thanks to the very narrow-band of the spike, the insertion loss at 12.8 GHz sensibly increases when losses are present. Of course, real filters have losses and if the insertion loss appears as a very narrow-band frequency response, it can be better suppressed considering lossy material in the simulation. Fig. 11 shows the  $S_{21}$  frequency response of the filter when aluminum losses were considered in the simulation. In this case, the insertion loss has been increased from 12 dB to 17 dB. Higher order  $TM_{120}$  mode parasitic band insertion loss is 30 dB. The first spurious appears at

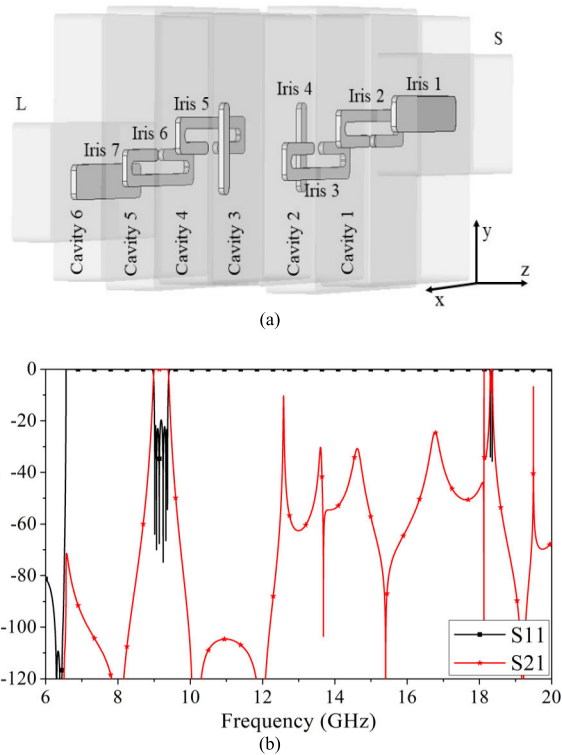


**FIGURE 10. Sixth order filter. (a) Filter configuration. (b) S-parameters response with wide bandwidth and wide spurious free band.**

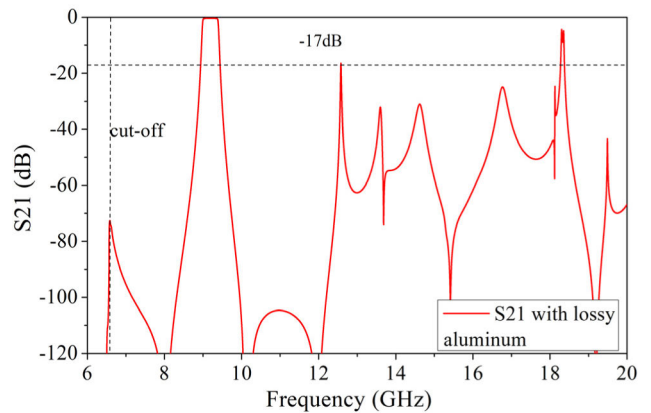


**FIGURE 11.  $S_{21}$  simulated frequency response when losses due to aluminum are considered.**

around 18 GHz. It means that the stopband for this wideband TM cavity filter is about 1.95 times the filter band center frequency of 9.2 GHz. The performance of the filter is better than that obtained with the method presented in [23] in terms of FBW and upper stopband performance. Fig. 12 shows the final positioning of the irises in the cavities. Table 1 provides the final optimized dimensions of the filter.

**IV. MEASUREMENT OF THE 6<sup>TH</sup> ORDER FILTER**

The proposed 6 pole TM cavity filter has been manufactured and measured. Photographs of assembled and disassembled filter are shown in Fig. 13(a) and Fig. 13(b),

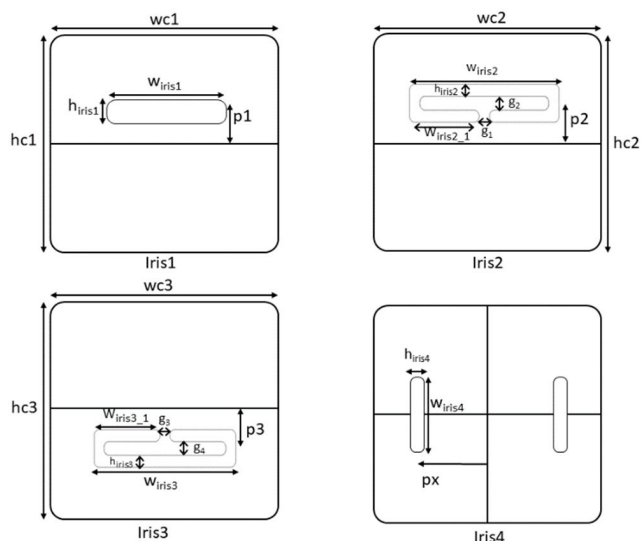


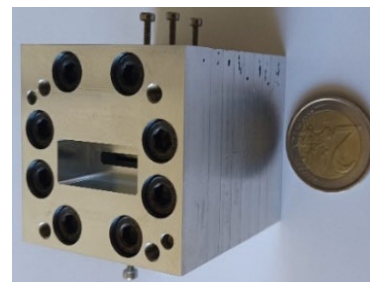
FIGURE 12. Final positioning of the irises in the cavities. The values of the parameters are reported in Table 1.

TABLE 1. Final optimized dimension of the filter.

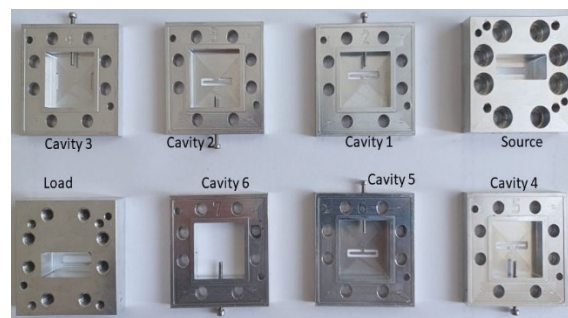
| Parameter  | Value (mm)   |
|------------|--|
| Iris 1 (7) | $w_{iris1}=14.74, h_{iris1}=3.03, p_1=2.85$                                      |
| Iris 2 (6) | $w_{iris2}=14.65, w_{iris2\_1}=6.825, h_{iris2}=1, g_1=1, g_2=1.15, p_2=2.5$     |
| Iris 3 (5) | $w_{iris3}=14.75, w_{iris3\_1}=6.275, h_{iris3}=1, g_3=2.2, g_4=1.15, p_3=-0.76$ |
| Iris 4     | $w_{iris4}=7.15, h_{iris4}=1.25, p_x=8.7$  |
| Cavity 1   | $w_{c1}=23.47, h_{c1}=22.86$   |
| Cavity 2   | $w_{c2}=23.47, h_{c2}=23.93$   |
| Cavity 3   | $w_{c3}=23.3, h_{c3}=22.95$  |

respectively. Tuning screws of radius 1 mm is inserted in each cavity. The comparison between simulated and measured in-band and wide range frequency responses are shown in Fig. 14(a) and Fig. 14(b), respectively. Filter band is centered at 9.2 GHz. However, the measured in-band return loss is slightly degraded at the lower edge of the band with respect to the simulations. The measured return loss is 18.5 dB and the insertion loss is around 0.5 dB. The measured stopband up to 18 GHz, has an insertion loss larger than 27 dB, this is better than the 17 dB in the simulation. The measured Q-factor is approximately 2000. The slight difference between simulated and measured frequency responses can be attributed to the manufacturing tolerances. Nevertheless, the measurement verifies the effectiveness of the proposed method.

Table 2 shows the comparison with other TM mode filter configurations reported in the technical literature in order to highlight the advantage of the wide out-of-band rejection performance of the proposed filter designs. Rosenberg *et al* in [16] shows the classical single mode TM cavity filter configuration with a FBW of 2.5%. Using capacitive irises, the stopband has been extended to 40 GHz, corresponding

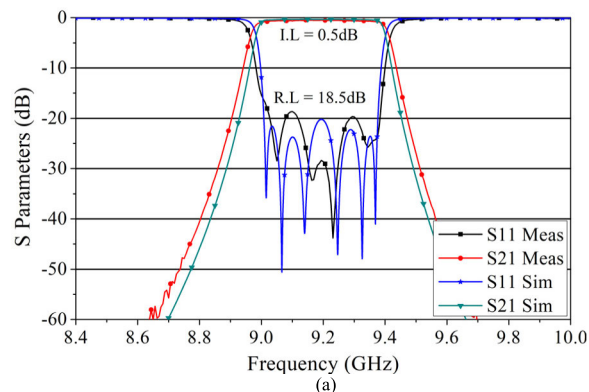


(a)

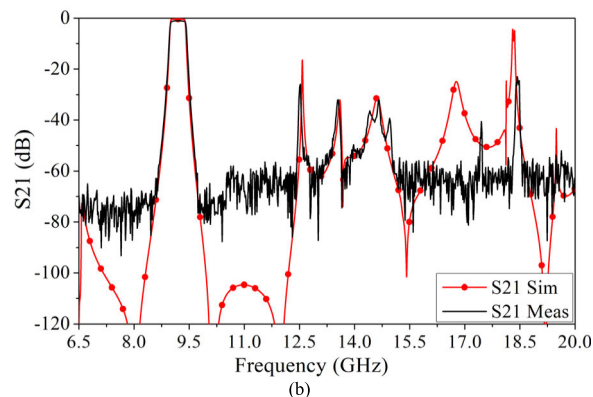


(b)

FIGURE 13. Fabricated photographs of the filter. (a) Assembled. (b) Disassembled.



(a)



(b)

FIGURE 14. Comparison between simulated and measured results. (a) In-band S parameter response. (b) Out-of-band S<sub>21</sub> response.

to 1.5 times the filter center frequency (27 GHz). However, use of capacitive irises results in the appearance of spurious resonances at the lower stopband region of the filter. In [18],

**TABLE 2.** Comparison with the previously published work.

| Reference        | Center frequency | Fractional bandwidth | Frequency of the first spurious | Ratio       |
|------------------|------------------|----------------------|---------------------------------|-------------|
| 2003 [16]        | 27 GHz           | 2.5%                 | 40 GHz                          | 1.5         |
| 2010 [18]        | 10 GHz           | 1.5%                 | 12.6 GHz                        | 1.26        |
| 2018 [20]        | 14.25 GHz        | 3.5%                 | 18 GHz                          | 1.27        |
| 2015 [21]        | 10 GHz           | 1.9%                 | 13.5 GHz                        | 1.35        |
| 2022 [23]        | 9.2 GHz          | 1.5%                 | 20.2 GHz                        | 2.2         |
| 2023 [25]        | 90 GHz           | 7.3%                 | 110 GHz                         | 1.23        |
| 2023 [26]        | 7.5 GHz          | 9.33%                | 9.5 GHz                         | 1.26        |
| <b>This work</b> | <b>9.2 GHz</b>   | <b>5%</b>            | <b>18 GHz</b>                   | <b>1.95</b> |

stopband performance has been achieved up to 12.6 GHz corresponding to 1.26 times the filter center frequency (10 GHz). Authors in [20] proposed a TM dual mode cavity filter achieving the stopband performance up to 18 GHz at the filter center frequency (14.25 GHz). Similarly, in [21] authors proposed different techniques used to improve stopband frequency response in TM dual mode cavity filters. However, frequency of the first spurious appears at 13.5 GHz. This corresponds to 1.35 times the filter center frequency (10 GHz). Bartlett et.al. in [25] and Bastioli et.al in [26] reported TM filters with wide FBW of 7.3% and 9.33% respectively. However, both the recent studies do not consider the wide out-of-band frequency response of the filter. Recently, in [23] by applying the spurious self-suppression method, TM cavity filter designs achieved improved stopband performance of up to 20.2 GHz corresponding to 2.2 times the filter center frequency (9.2 GHz), with a FBW of 1.5%. In this context, this paper extends the contribution of [23] and presents TM cavity filter designs with wide passbands and improved stopband performance by removing TE<sub>10</sub> mode iris resonances. TM filters can be designed up to FBW of 5% with wide spurious free range up to 18 GHz corresponding to 1.95 times at the filter center frequency of 9.2 GHz.

## V. CONCLUSION

In this paper, compact TM cavity filters with wide bandwidth and wide spurious free range have been presented. In particular, it has been shown how to achieve the maximum obtainable bandwidth of TM filter with wide stopbands. Indeed, according to [23], TM filters with wide stopband performance cannot reach wide passbands because of the iris resonances that degrade the stopband performance. However, this problem can be solved by replacing conventional rectangular iris with the proposed bent c-shaped iris. The main contributions of this paper are: 1) Removing spurious frequencies due to the TE<sub>10</sub> mode of coupling irises, thus improving the stopband performance of the filters. 2) Increasing the FBW of the filters. It has also been shown that, by carefully considering the out-of-band requirements, filters can be designed up to FBW of 5%. Examples of 4<sup>th</sup> order and 6<sup>th</sup> order TM cavity filters having the FBW of 5% and 4% respectively, are presented in this paper. Finally, in order to demonstrate the feasibility of

the proposed approach, the 6<sup>th</sup> order TM cavity filter has been manufactured and measured. Measured results shows good agreement with the simulation.

## REFERENCES

- [1] R. V. Snyder, A. Mortazawi, I. Hunter, S. Bastioli, G. Macchiarella, and K. Wu, "Present and future trends in filters and multiplexers," *IEEE Trans. Microw. Theory Techn.*, vol. 63, no. 10, pp. 3324–3360, Oct. 2015.
- [2] R. Levy, R. V. Snyder, and G. Matthaei, "Design of microwave filters," *IEEE Trans. Microw. Theory Techn.*, vol. 50, no. 3, pp. 783–793, Mar. 2002.
- [3] V. Boria and B. Gimeno, "Waveguide filters for satellites," *IEEE Microw. Mag.*, vol. 8, no. 5, pp. 60–70, Oct. 2007.
- [4] R. V. Snyder, G. Macchiarella, S. Bastioli, and C. Tomassoni, "Emerging trends in techniques and technology as applied to filter design," *IEEE J. Microw.*, vol. 1, no. 1, pp. 317–344, Jan. 2021.
- [5] G. Goussetis and D. Budimir, "Integration of lowpass filters in bandpass filters for stopband improvement," in *Proc. 32nd Eur. Microw. Conf.*, Sep. 2002, pp. 1–3.
- [6] Q. Wu, F. Zhu, Y. Yang, and X. Shi, "An effective approach to suppressing the spurious mode in rectangular waveguide filters," *IEEE Microw. Wireless Compon. Lett.*, vol. 29, no. 11, pp. 703–705, Nov. 2019.
- [7] M. Morelli, I. Hunter, R. Parry, and V. Postoyalko, "Stopband performance improvement of rectangular waveguide filters using stepped-impedance resonators," *IEEE Trans. Microw. Theory Techn.*, vol. 50, no. 7, pp. 1657–1664, Jul. 2002.
- [8] M. Morelli, I. Hunter, R. Parry, and V. Postoyalko, "Stop-band improvement of rectangular waveguide filters using different width resonators: Selection of resonator widths," in *IEEE MTT-S Int. Microw. Symp. Dig.*, May 2001, pp. 1623–1626.
- [9] J. Valencia, V. E. Boria, M. Guglielmi, and S. Cogollos, "Compact wideband hybrid filters in rectangular waveguide with enhanced out-of-band response," *IEEE Trans. Microw. Theory Techn.*, vol. 68, no. 1, pp. 87–101, Jan. 2020.
- [10] J. Valencia, M. Guglielmi, S. Cogollos, J. Vague, and V. E. Boria, "Enhancing the performance of stepped impedance resonator filters in rectangular waveguide," in *Proc. 47th Eur. Microw. Conf. (EuMC)*, Oct. 2017, pp. 989–992.
- [11] J. F. Valencia Sullca, M. Guglielmi, S. Cogollos, and V. E. Boria, "Hybrid wideband staircase filters in rectangular waveguide with enhanced out-of-band response," *IEEE Trans. Microw. Theory Techn.*, vol. 69, no. 8, pp. 3783–3796, Aug. 2021.
- [12] R. J. Cameron, C. M. Kudsia, and R. R. Mansour, *Microwave Filters for Communication System: Fundamentals Design and Applications*, 2nd ed. Hoboken, NJ, USA: Wiley, 2018.
- [13] M. Guglielmi, F. Montauti, L. Pellegrini, and P. Arcioni, "Implementing transmission zeros in inductive-window bandpass filters," *IEEE Trans. Microw. Theory Techn.*, vol. 43, no. 8, pp. 1911–1915, Aug. 1995.
- [14] C. Carceller, P. Soto, V. E. Boria, and M. Guglielmi, "Design of hybrid folded rectangular waveguide filters with transmission zeros below the passband," *IEEE Trans. Microw. Theory Techn.*, vol. 64, no. 2, pp. 475–485, Feb. 2016.
- [15] C. Carceller, P. Soto, V. Boria, M. Guglielmi, and D. Raboso, "New folded configuration of rectangular waveguide filters with asymmetrical transmission zeros," in *Proc. 44th Eur. Microw. Conf.*, Oct. 2014, pp. 183–186.
- [16] U. Rosenberg, S. Amari, and J. Bornemann, "Inline TM<sub>110</sub> mode filters with high-design flexibility by utilizing bypass couplings of nonresonating TE<sub>10</sub>01 modes 110-mode filters with high-design flexibility by utilizing bypass couplings of nonresonating TE<sub>10</sub>01 modes," *IEEE Trans. Microw. Theory Techn.*, vol. 51, no. 6, pp. 1735–1742, Jun. 2003.
- [17] S. Bastioli, "Nonresonating mode waveguide filters," *IEEE Microw. Mag.*, vol. 12, no. 6, pp. 77–86, Oct. 2011.
- [18] S. Bastioli, C. Tomassoni, and R. Sorrentino, "A new class of waveguide dual-mode filters using TM and nonresonating modes," *IEEE Trans. Microw. Theory Techn.*, pp. 3909–3917, Dec. 2010.
- [19] C. Tomassoni, S. Bastioli, and R. Sorrentino, "Generalized TM dual-mode cavity filters," *IEEE Trans. Microw. Theory Techn.*, vol. 59, no. 12, pp. 3338–3346, Dec. 2011.
- [20] L. Pelliccia, C. Tomassoni, F. Cacciamani, P. Vallerotonda, R. Sorrentino, J. Galdeano, and C. Ernst, "Very-compact waveguide bandpass filter based on dual-mode TM cavities for satellite applications in Ku-band," in *Proc. 48th Eur. Microw. Conf. (EuMC)*, Sep. 2018, pp. 93–96.



- [21] C. Tomassoni, M. Dionigi, and R. Sorrentino, "Strategies for the improvement of the out of band behavior of TM dual-mode filters," in *Proc. IEEE 1st Int. Forum Res. Technol. Soc. Ind. Leveraging Better Tomorrow (RTSI)*, Sep. 2015, pp. 90–93.
- [22] A. Rehman and C. Tomassoni, "Spurious suppression through the control of their couplings: Application to TM cavity filters," in *IEEE MTT-S Int. Microw. Symp. Dig.*, Jun. 2021, pp. 150–153.
- [23] A. Rehman and C. Tomassoni, "Spurious self-suppression method: Application to TM cavity filters," *IEEE Trans. Microw. Theory Techn.*, vol. 71, no. 3, pp. 1201–1215, Mar. 2023.
- [24] A. Rehman, C. Tomassoni, L. Silvestri, M. Bozzi, N. Delmonte, and L. Perregini, "Self cancellation of higher order mode spurious frequencies in SIW filters," in *IEEE MTT-S Int. Microw. Symp. Dig.*, Nov. 2021, pp. 339–342.
- [25] C. Bartlett, J. Bornemann, and M. Höft, "Improved TM dual-mode filters with reduced fabrication complexity," *IEEE J. Microw.*, vol. 3, no. 1, pp. 60–69, Jan. 2023.
- [26] S. Bastioli, R. Snyder, C. Tomassoni, and V. D. L. Rubia, "Direct-coupled TE–TM waveguide cavities," *IEEE Microw. Wireless Technol. Lett.*, early access, Apr. 10, 2023, doi: [10.1109/LMWT.2023.3263905](https://doi.org/10.1109/LMWT.2023.3263905).



**CRISTIANO TOMASSONI** (Senior Member, IEEE) received the Ph.D. degree in electronics engineering from the University of Perugia, Perugia, Italy, in 1999.

In 1999, he joined as a Visiting Scientist and the Lehrstuhl für Hochfrequenztechnik, Technical University of Munich, Munich, Germany, where he was involved in the modeling of waveguide structures and devices by using the generalized scattering matrix technique. In 2001, he joined the Fakultät für Elektrotechnik und Informationstechnik, Otto-von-Guericke University, Magdeburg, Germany, as a Guest Professor. During his early career, he studied and contributed the enhancement of several analytical and numerical methods for the simulation of electromagnetic components, such as finite-element method, mode-matching technique, generalized multipole technique, method of moments, transmission-line matrix, and mode matching applied to the spherical waves. In 2007, he became an Assistant Professor with the University of Perugia, where he is currently an Associate Professor and he teaches the "electromagnetic fields" and "advanced design of microwave and RF systems" courses. His research interests include the modeling and design of waveguide devices and antennas, the development of miniaturized filters, reconfigurable filters, dielectric filters, substrate integrated waveguide filters, and 3-D printed filters. He was a recipient of the Best Paper Award (second place) from the International Conference on Numerical, Electromagnetic and Multiphysics Modeling and Optimization (NEMO 2018), the Best Paper Award (first place) from the 15th Mediterranean Microwave Symposium (MMS2015), and the 2012 Microwave Prize presented by the IEEE Microwave Theory and Technique Society. He is the Vice-Chair of the MTT-5 Filters and Passive Components Technical Committee. He was an Associate Editor of the *IEEE TRANSACTIONS ON MICROWAVE THEORY AND TECHNIQUE*, from 2019 to 2022.

...



**ABDUL REHMAN** was born in Islamabad, Pakistan, in 1991. He received the B.S. degree in electronics engineering from Muhammad Ali Jinnah University, Islamabad, in 2013, and the master's degree in information and communication engineering from Incheon National University, Incheon, South Korea, in 2018. He is currently pursuing the Ph.D. degree in electronic and information engineering with the University of Perugia, Italy.

He was a Research Associate with COMSATS University Islamabad (CUI), Islamabad, from 2014 to 2016, and in 2018 and 2019. His research interests include the designing of passive microwave components using waveguide, substrate integrated waveguide (SIW) technologies, the design of high performance, wide stopband, and miniaturized microwave filters.